Cryptand derived fluorescence signaling systems for sensing Hg(II) ion : a comparative study

Kalyan K. Sadhu, Susan Sen and Parimal K. Bharadwaj[*]

Chemistry Department, Indian Institute of Technology Kanpur, 208016 India

Email: pkb@iitk.ac.in

Supporting Information

Captions for the Figures and Tables:

Fig. S1:	ESI-MS spectrum of $\mathbf{L_3}$.
Fig. S2:	500 MHz ^{1}H-NMR spectrum of $\mathbf{L_3}$.
Fig. S3:	125 MHz ^{13}C-NMR spectrum of $\mathbf{L_3}$.
Fig. S4:	ESI-MS spectrum of $\mathbf{L_7}$.
Fig. S5:	500 MHz ^{1}H-NMR spectrum of $\mathbf{L_7}$.
Fig. S6:	125 MHz ^{13}C-NMR spectrum of $\mathbf{L_7}$.
Fig. S7:	ESI-MS spectrum of $\mathbf{L_8}$.
Fig. S8:	500 MHz ^{1}H-NMR spectrum of $\mathbf{L_8}$.
Fig. S9:	125 MHz ^{13}C-NMR spectrum of $\mathbf{L_8}$.
Fig. S10:	ESI-MS spectrum of $\mathbf{L_9}$.
Fig. S11:	500 MHz ^{1}H-NMR spectrum of $\mathbf{L_9}$.
Fig. S12:	125 MHz ^{13}C-NMR spectrum of $\mathbf{L_9}$.
Table ST1A:	Absorption and molar extinction coefficient (ε) of $\mathbf{L_1}$ alone and in presence of different metal ions in MeCN.
Table ST1B	Absorption and molar extinction coefficient (ε) of $\mathbf{L_7}$ alone and in presence of different metal ions in MeCN.
Table ST2A:	Absorption and molar extinction coefficient (ε) of $\mathbf{L_2}$ alone and in presence of different metal ions in MeCN.

Table ST2B: Absorption and molar extinction coefficient (ε) of $\mathbf{L_8}$ alone and in presence of different metal ions in MeCN.

Table ST3A: Absorption and molar extinction coefficient (ε) of $\mathbf{L_3}$ alone and in presence of different metal ions in MeCN.

Table ST3B: Absorption and molar extinction coefficient (ε) of $\mathbf{L_9}$ alone and in presence of different metal ions in MeCN.

Fig. S13A-S15A: Absorption spectra of $\mathbf{L_1}$, $\mathbf{L_2}$ and $\mathbf{L_3}$ in presence of different ionic inputs in MeCN.

Fig. S13B-S15B: Absorption spectra of $\mathbf{L_7}$, $\mathbf{L_8}$ and $\mathbf{L_9}$ in presence of different ionic inputs in MeCN.

Table ST4: Absorption and molar extinction coefficient (ε) of $\mathbf{L_4}$ alone and in presence of different metal ions in MeCN.

Table ST5: Absorption and molar extinction coefficient (ε) of $\mathbf{L_5}$ alone and in presence of different metal ions in MeCN.

Table ST6: Absorption and molar extinction coefficient (ε) of $\mathbf{L_6}$ alone and in presence of different metal ions in MeCN.

Table ST7A: Fluorescence output of $\mathbf{L_1}$-$\mathbf{L_3}$ with different ionic inputs.

Table ST7B: Fluorescence output of $\mathbf{L_7}$-$\mathbf{L_9}$ with different ionic inputs.

Fig. S16: Absorption spectra of $\mathbf{L_1}$ in presence of increasing concentration of Hg(II) ionic inputs in MeCN.

Fig. S17-S19: Absorption and emission spectra of $\mathbf{L_2}$ in presence of increasing concentration of Hg(II) ionic inputs and plots of fluorescence quantum yield of $\mathbf{L_2}$ as a function of concentration of Hg(II) added in MeCN.

Fig. S20-S22: Absorption and emission spectra of $\mathbf{L_3}$ in presence of increasing concentration of Hg(II) ionic inputs and plots of fluorescence quantum yield of $\mathbf{L_3}$ as a function of concentration of Hg(II) added in MeCN.

Fig. S23-S24: Linear regression plots for complex stability constant determination of $\mathbf{L_2}$ and $\mathbf{L_3}$ in presence of Hg(II) as ionic input in MeCN.

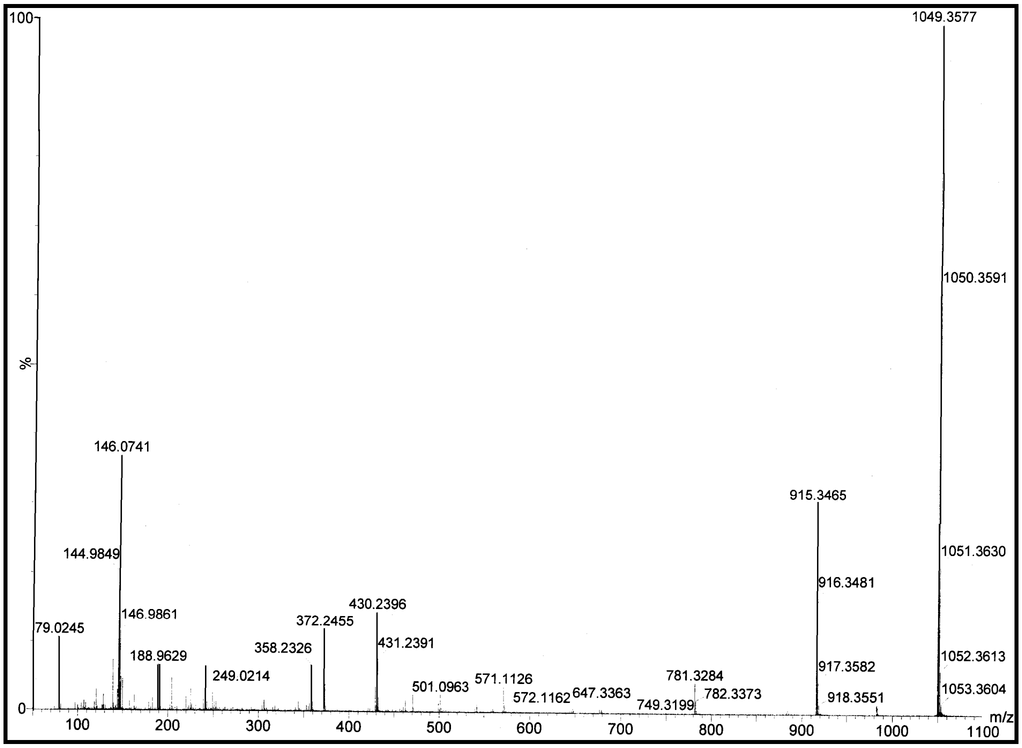

Fig. S1: ESI-MS spectrum of $\mathbf{L_3}$.

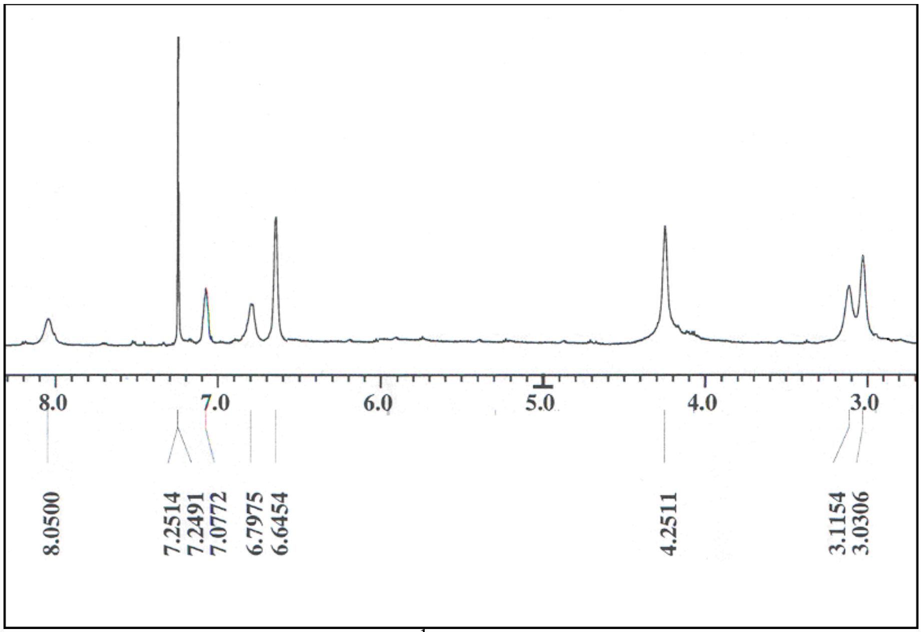

Fig. S2: 500 MHz ^{1}H-NMR spectrum of $\mathbf{L_3}$.

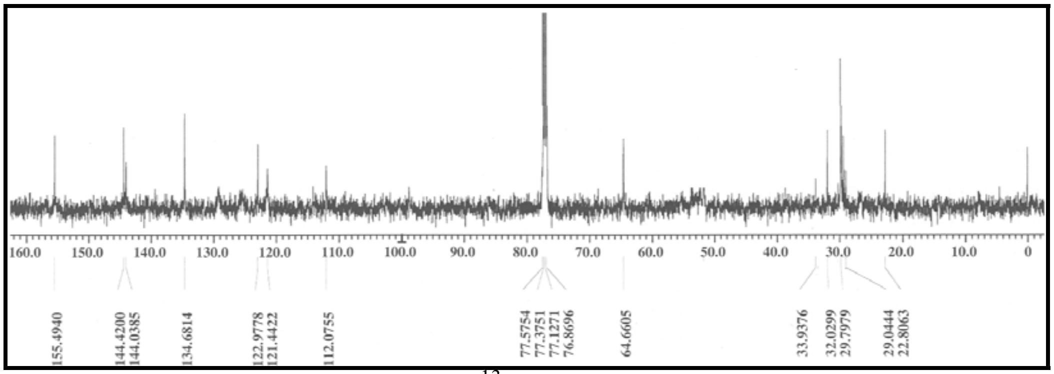

Fig. S3: 125 MHz ^{13}C-NMR spectrum of **L$_3$**.

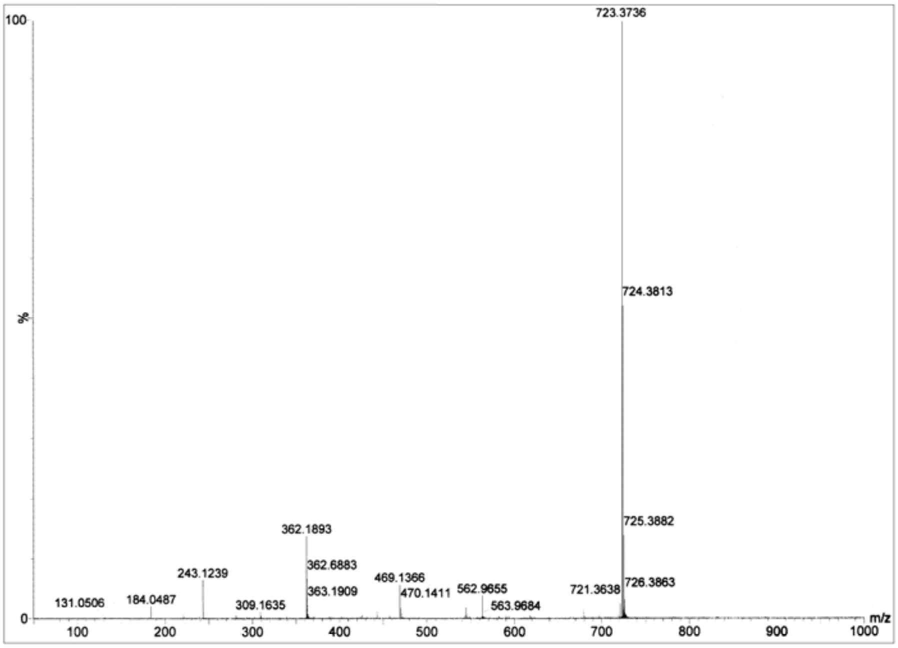

Fig. S4: ESI-MS spectrum of **L$_7$**.

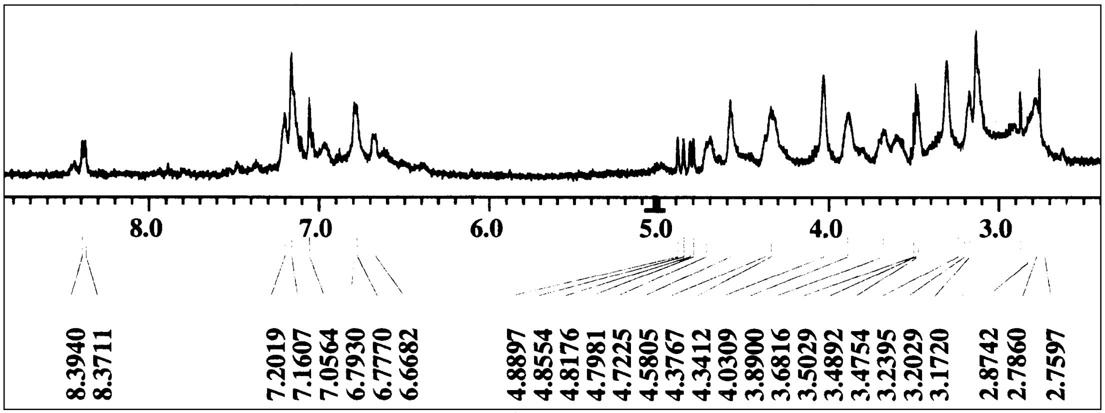

Fig. S5: 500 MHz ^{1}H-NMR spectrum of **L**$_7$.

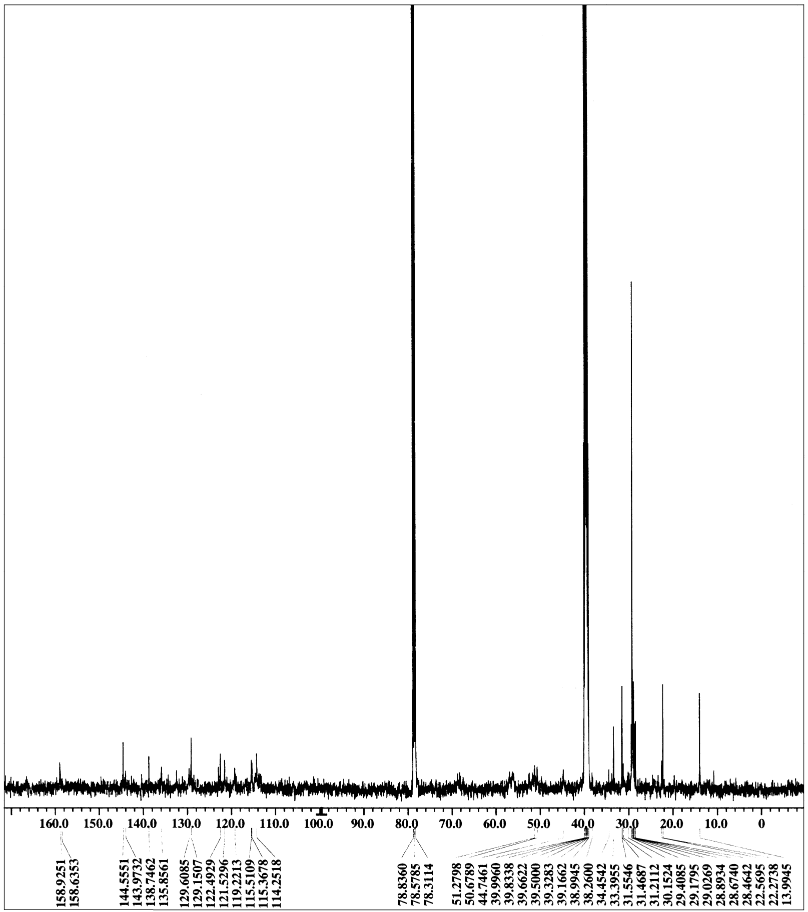

Fig. S6: 125 MHz ^{13}C-NMR spectrum of **L**$_7$.

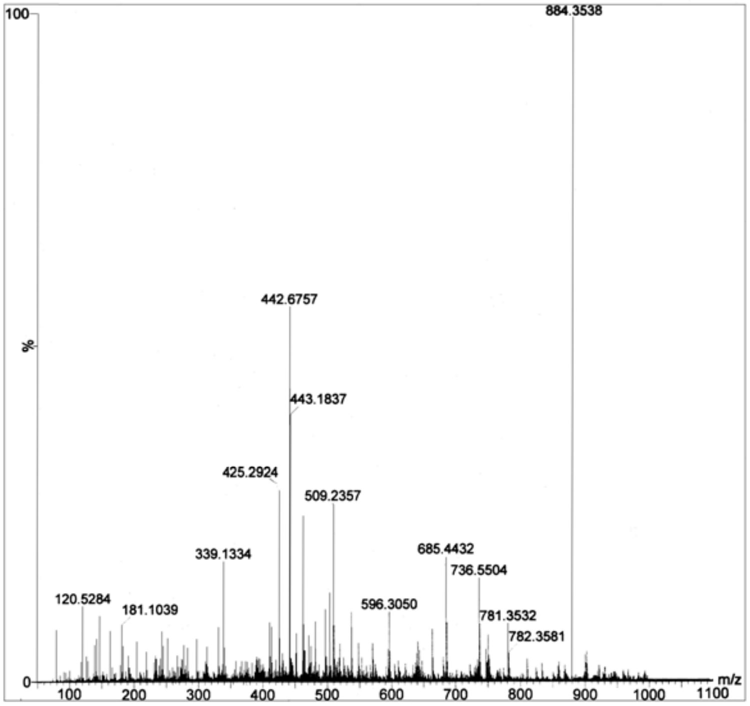

Fig. S7: ESI-MS spectrum of $\mathbf{L_8}$

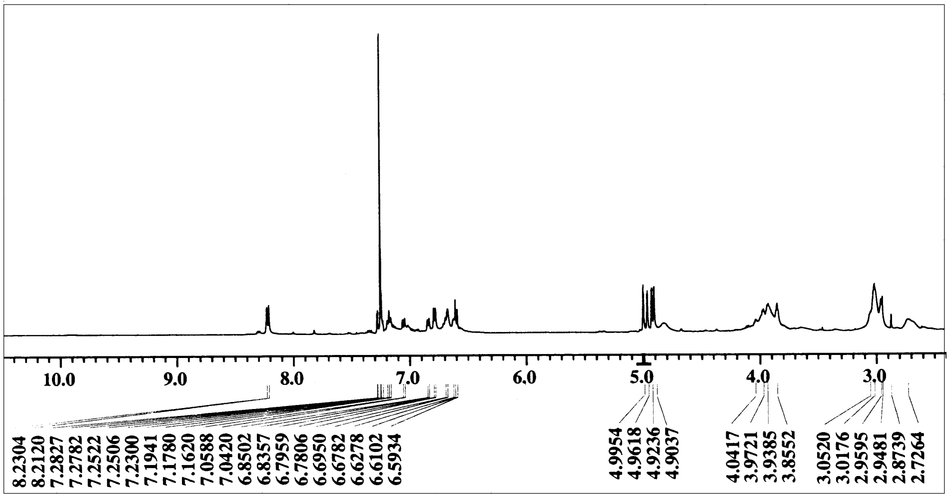

Fig. S8: 500 MHz ^{1}H-NMR spectrum of $\mathbf{L_8}$.

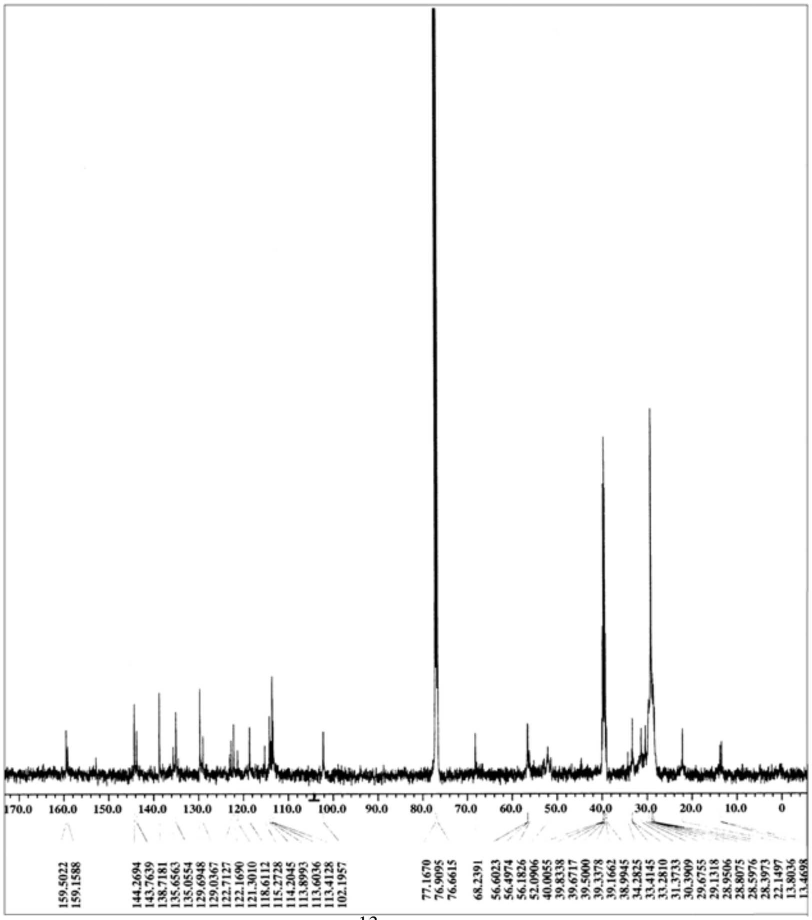

Fig. S9: 125 MHz ^{13}C-NMR spectrum of $\mathbf{L_8}$.

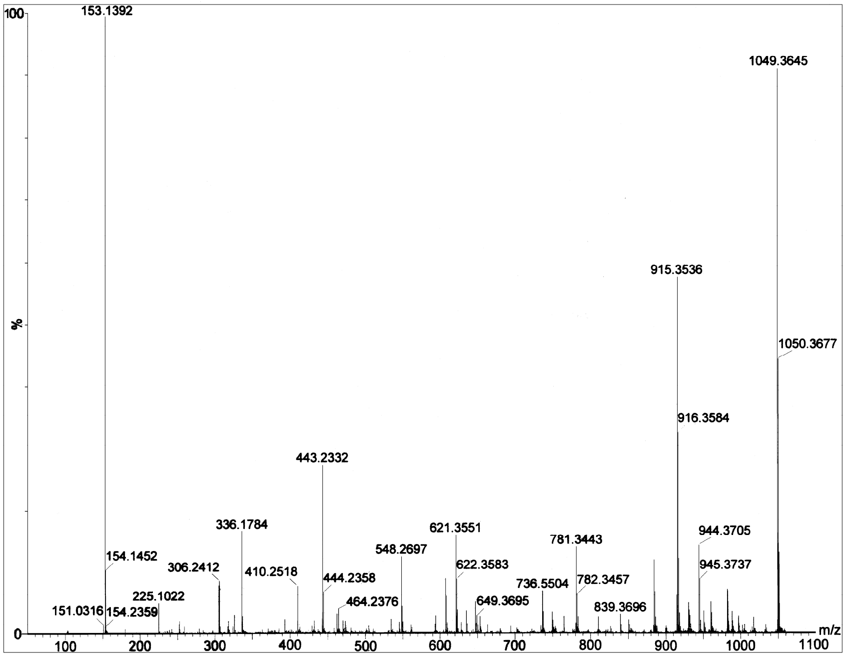

Fig. S10: ESI-MS spectrum of $\mathbf{L_9}$

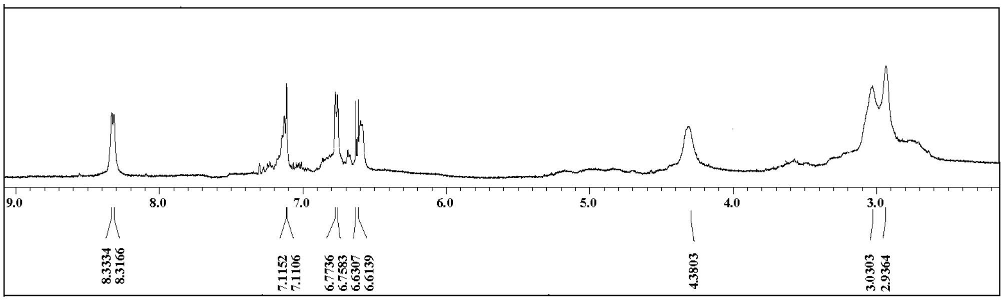

Fig. S11: 500 MHz ^{1}H-NMR spectrum of **L$_9$**.

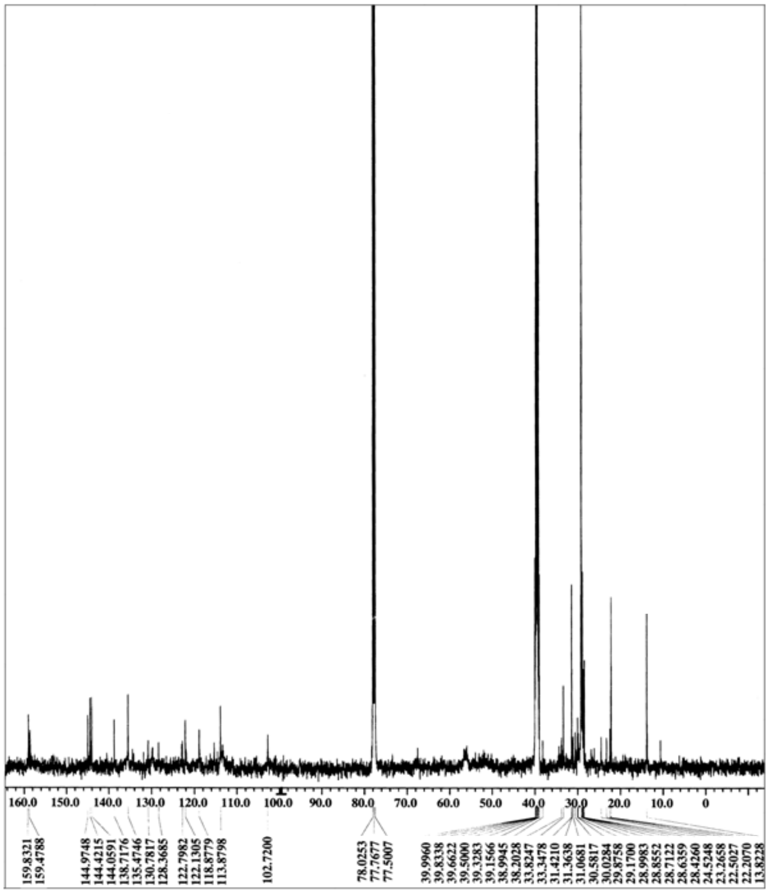

Fig. S12: 125 MHz ^{13}C-NMR spectrum of **L$_9$**.

Table ST1A: Absorption and molar extinction coefficient (ε) of $\mathbf{L_1}$ alone and in presence of different metal ions in MeCN. Conc. of $\mathbf{L_1}$ = 1.15 × 10^{-5} (M)

	Absorption λ, nm (ε, dm^3 mol^{-1} cm^{-1})	
$\mathbf{L_1}$	483 (12470)	342 (5434)
$\mathbf{L_1}$+Cd(II)	479 (12478)	339 (5357)
$\mathbf{L_1}$+Hg(II)	465 (11130)	331 (4826)

Table ST1B Absorption and molar extinction coefficient (ε) of $\mathbf{L_7}$ alone and in presence of different metal ions in MeCN. Conc. of $\mathbf{L_7}$ = 1.056 × 10^{-5} (M)

	Absorption λ, nm (ε, dm^3 mol^{-1} cm^{-1})		
$\mathbf{L_7}$	482 (15915)	343(5773)	277 (2724)
$\mathbf{L_7}$+Mn(II)	479 (16812)	341 (6184)	274 (2473)
$\mathbf{L_7}$+Fe(II)	454 (6116)	354 (18029)	273 (14679)
$\mathbf{L_7}$+Co(II)	472 (22881)	334 (4773)	275 (1893)
$\mathbf{L_7}$+Ni(II)	478 (14830)	347 (5354)	274 (1473)
$\mathbf{L_7}$+Cu(II)	457 (8234)	321 (3309)	
$\mathbf{L_7}$+Zn(II)	473 (14856)	339 (5088)	274 (2177)
$\mathbf{L_7}$+Cd(II)	477 (15032)	343 (6241)	276 (2493)
$\mathbf{L_7}$+Ag(I)	469(14419)	334 (4718)	275 (1828)
$\mathbf{L_7}$+Hg(II)	469 (12356)	334 (2846)	
$\mathbf{L_7}$+Pb(II)	469 (9311)	334 (1497)	272 (3362)
$\mathbf{L_7}$+H^+	464(13478)	331 (3854)	270 (1479)

Table ST2A: Absorption and molar extinction coefficient (ε) of **L$_2$** alone and in presence of different metal ions in MeCN. Conc. of **L$_2$** = 4.12 × 10^{-5} (M)

	Absorption λ, nm (ε, dm^3 mol^{-1} cm^{-1})		
L$_2$	486 (24544)	342 (9687)	272 (4614)
L$_2$+Mn(II)	479 (23813)	338 (9211)	271 (4158)
L$_2$+Fe(II)	452 (16910)	321 (8813)	275 (5177)
L$_2$+Co(II)	475 (25805)	335 (9211)	268 (4150)
L$_2$+Ni(II)	479 (23711)	341 (9339)	272 (4107)
L$_2$+Cu(II)	453 (17643)	321 (8653)	
L$_2$+Zn(II)	474 (23532)	336 (9313)	267 (4284)
L$_2$+Cd(II)	479 (24000)	341 (9294)	272 (4131)
L$_2$+Ag(I)	484 (25883)	341 (9774)	272 (4456)
L$_2$+Hg(II)	469 (21886)	333 (8498)	276 (3881)
L$_2$+Pb(II)	478 (23580)	335 (10051)	272 (6995)
L$_2$+H$^+$	456 (21541)	328 (8641)	270 (4694)

Table ST2B: Absorption and molar extinction coefficient (ε) of **L$_8$** alone and in presence of different metal ions in MeCN. Conc. of **L$_8$** = 0.997 × 10^{-5} (M)

	Absorption λ, nm (ε, dm^3 mol^{-1} cm^{-1})		
L$_8$	483 (36074)	341(11704)	273 (7227)
L$_8$+Mn(II)	479 (32585)	338 (9977)	271 (5196)
L$_8$+Fe(II)	461 (26158)	353 (63976)	274(59314)
L$_8$+Co(II)	477 (40220)	337 (10545)	277 (8330)
L$_8$+Ni(II)	481(35690)	341 (11668)	270 (5878)
L$_8$+Cu(II)	453 (21885)	294(18245)	
L$_8$+Zn(II)	474 (24565)	336(7239)	271 (4571)
L$_8$+Cd(II)	479 (31277)	340 (9434)	271(4721)
L$_8$+Ag(I)	463(26842)	334 (8258)	275 (5320)
L$_8$+Hg(II)	461 (29895)	327 (9447)	
L$_8$+Pb(II)	461 (27928)	327 (11109)	
L$_8$+H$^+$	462(29335)	327 (9278)	270 (6755)

Table ST3A: Absorption and molar extinction coefficient (ε) of $\mathbf{L_3}$ alone and in presence of different metal ions in MeCN. Conc. of $\mathbf{L_3}$ = 3.2×10^{-5} (M)

	Absorption λ, nm (ε, $dm^3\ mol^{-1}\ cm^{-1}$)		
$\mathbf{L_3}$	482 (32953)	337 (12147)	267 (5097)
$\mathbf{L_3}$+Mn(II)	483 (31181)	337 (11150)	269 (4750)
$\mathbf{L_3}$+Fe(II)	466 (24575)	330 (11288)	274 (5540)
$\mathbf{L_3}$+Co(II)	477 (33456)	335 (11559)	267 (4716)
$\mathbf{L_3}$+Ni(II)	480 (32269)	337 (11716)	267 (4806)
$\mathbf{L_3}$+Cu(II)	455 (24475)	321 (11634)	
$\mathbf{L_3}$+Zn(II)	477 (31138)	336 (11581)	264 (4916)
$\mathbf{L_3}$+Cd(II)	480 (30663)	337 (11025)	267 (4428)
$\mathbf{L_3}$+Ag(I)	487 (30063)	340 (10675)	271 (4809)
$\mathbf{L_3}$+Hg(II)	472 (28850)	333 (11181)	
$\mathbf{L_3}$+Pb(II)	477 (31500)	335 (12709)	275 (7631)
$\mathbf{L_3}$+H^+	460 (27694)	327 (11253)	270 (5588)

Table ST3B: Absorption and molar extinction coefficient (ε) of $\mathbf{L_9}$ alone and in presence of different metal ions in MeCN. Conc. of $\mathbf{L_9}$ = 1.0715×10^{-5} (M)

	Absorption λ, nm (ε, $dm^3\ mol^{-1}\ cm^{-1}$)		
$\mathbf{L_9}$	483 (42702)	341(16583)	274 (7896)
$\mathbf{L_9}$+Mn(II)	481(44962)	340 (16330)	270 (7560)
$\mathbf{L_9}$+Fe(II)	449 (24340)	350 (56891)	273(56426)
$\mathbf{L_9}$+Co(II)	470 (39863)	333(12602)	270 (7195)
$\mathbf{L_9}$+Ni(II)	483(44683)	339 (16801)	269(7752)
$\mathbf{L_9}$+Cu(II)	454 (22860)	294(13075)	
$\mathbf{L_9}$+Zn(II)	481 (37777)	337(13844)	270 (6911)
$\mathbf{L_9}$+Cd(II)	473 (3646)	337 (12929)	270(5917)
$\mathbf{L_9}$+Ag(I)	463(29783)	328 (11318)	270 (5851)
$\mathbf{L_9}$+Hg(II)	461 (26517)	327 (10403)	
$\mathbf{L_9}$+Pb(II)	473 (30672)	330 (14632)	
L9+H^+	462(32452)	327 (12940)	270 (8574)

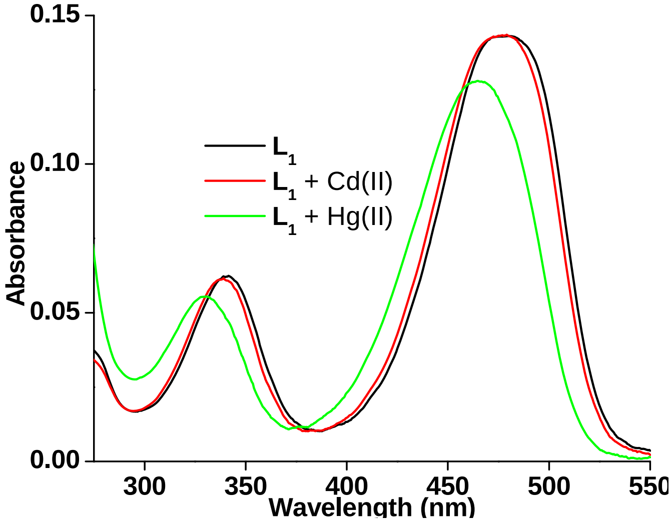

Fig. S13A: Absorption spectra of $\mathbf{L_1}$ in presence of different ionic inputs in MeCN.

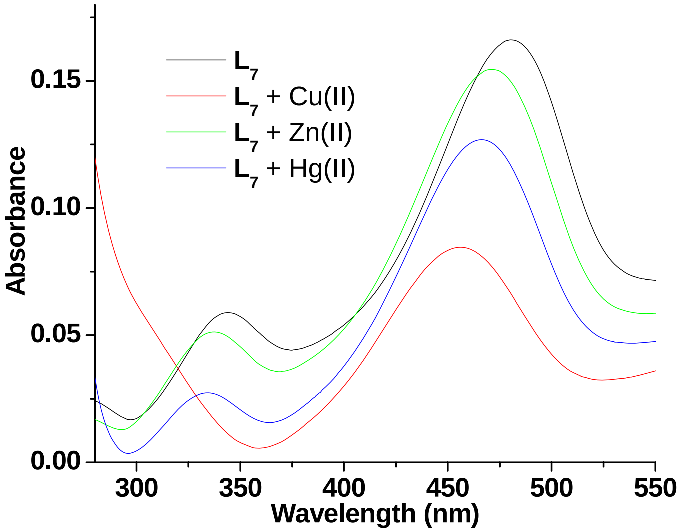

Fig. S13B: Absorption spectra of $\mathbf{L_7}$ in presence of different ionic inputs in MeCN.

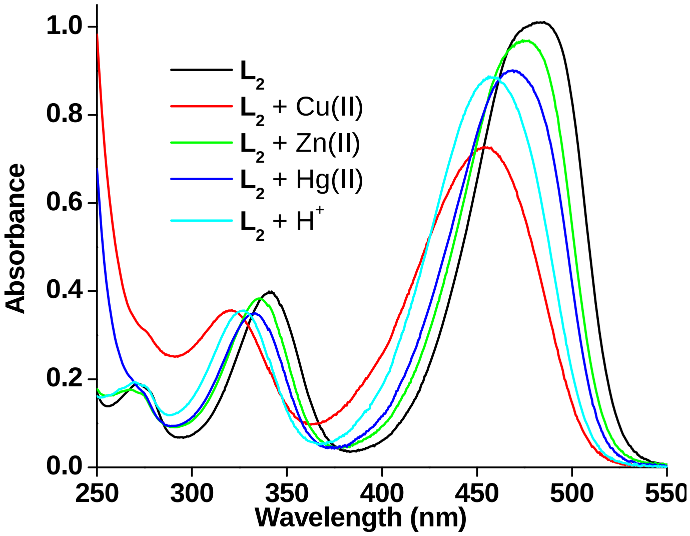

Fig. S14A: Absorption spectra of $\mathbf{L_2}$ in presence of different ionic inputs in MeCN.

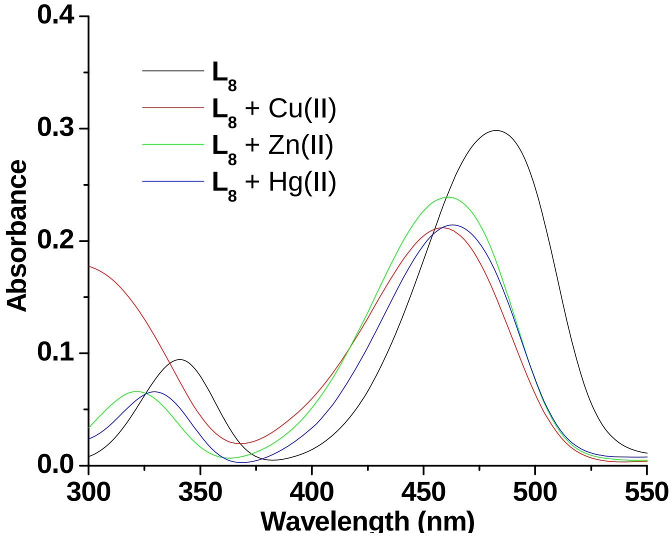

Fig. S14B: Absorption spectra of $\mathbf{L_8}$ in presence of different ionic inputs in MeCN.

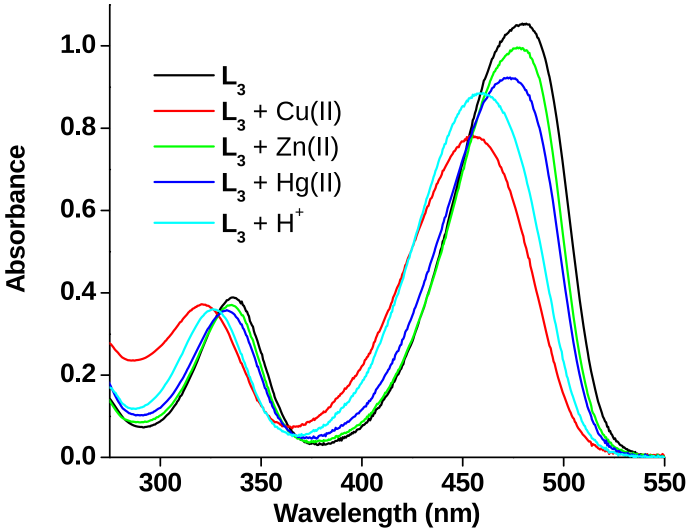

Fig. S15A: Absorption spectra of $\mathbf{L_3}$ in presence of different ionic inputs in MeCN.

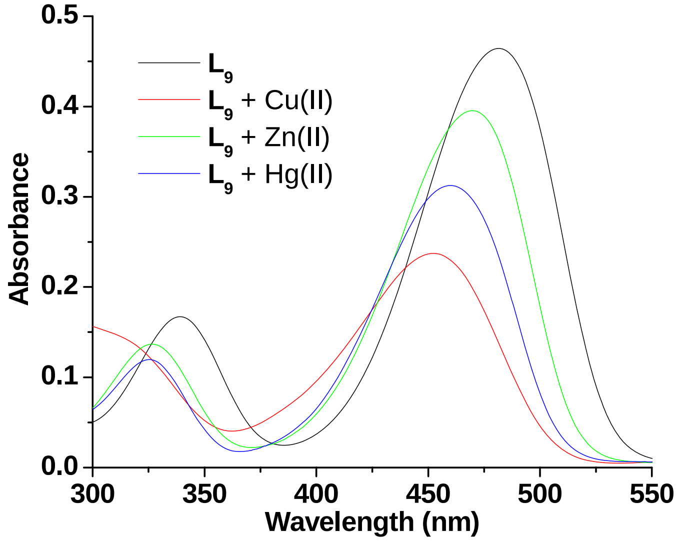

Fig. S15B: Absorption spectra of $\mathbf{L_9}$ in presence of different ionic inputs in MeCN.

Table ST4: Absorption and molar extinction coefficient (ε) of **L_4** alone and in presence of different metal ions in MeCN. Conc. of **L_4** = 5.0×10^{-5} (M)

	Absorption λ, nm (ε, $dm^3\ mol^{-1}\ cm^{-1}$)				
L_4	387 (6956)	367 (7828)	349 (5010)	332 (2698)	317 (1564)
L_4+Zn(II)	390 (5734)	370 (6642)	353 (4748)	335 (2668)	320 (1598)
L_4+Hg(II)	392 (5344)	373 (6424)	355 (4942)	335 (2712)	321 (1744)

Table ST5: Absorption and molar extinction coefficient (ε) of **L_5** alone and in presence of different metal ions in MeCN. Conc. of **L_5** = 1.42×10^{-5} (M)

	Absorption λ, nm (ε, $dm^3\ mol^{-1}\ cm^{-1}$)				
L_5	387 (13563)	367 (13683)	350 (9514)	333 (6296)	318 (1564)
L_5+Zn(II)	389 (12817)	370 (13021)	352 (9261)	335 (5641)	
L_5+Hg(II)	391 (12789)	371 (13261)	354 (9951)	334 (6147)	

Table ST6: Absorption and molar extinction coefficient (ε) of **L_5** alone and in presence of different metal ions in MeCN. Conc. of **L_6** = 0.95×10^{-5} (M)

	Absorption λ, nm (ε, $dm^3\ mol^{-1}\ cm^{-1}$)				
L_6	390 (20916)	370 (24653)	352 (18305)	334 (11832)	318 (7758)
L_6+Zn(II)	391 (21832)	371 (25768)	352 (18537)	337 (10863)	320 (6316)
L_6+Hg(II)	392 (19453)	373 (24232)	354 (18600)	336 (10484)	

Table ST7A: Fluorescence output of $\mathbf{L_1}$-$\mathbf{L_3}$ with different ionic inputs.

Inputs	Quantum Yield ϕ (Enhancement Factor) (λ_{ex}= 345 nm)		
	$\mathbf{L_1}$ ϕ	$\mathbf{L_2}$ ϕ	$\mathbf{L_3}$ ϕ
None	0.002	0.003	0.004
Mn(II)	0.120 (60)	0.185 (62)	0.251 (63)
Fe(II)	0.100 (50)	0.157 (52)	0.232 (58)
Co(II)	0.096 (48)	0.176 (59)	0.267 (67)
Ni(II)	0.076 (38)	0.154 (51)	0.244 (61)
Cu(II)	0.084 (42)	0.170 (57)	0.302 (76)
Zn(II)	0.190 (95)	0.289 (96)	0.412 (103)
Cd(II)	0.427 (214)	0.418 (139)	0.377 (94)
Ag(I)	0.170 (85)	0.269 (90)	0.341 (85)
Hg(II)	0.868 (434)	0.746 (249)	0.508 (127)
Pb(II)	0.340 (170)	0.514 (165)	0.446 (112)
H^+	0.060 (30)	0.085 (28)	0.095 (24)

Table ST7B: Fluorescence output of $\mathbf{L_7}$-$\mathbf{L_9}$ with different ionic inputs.

Inputs	Quantum Yield ϕ (Enhancement Factor) (λ_{ex}= 345 nm)		
	$\mathbf{L_7}$ ϕ	$\mathbf{L_8}$ ϕ	$\mathbf{L_9}$ ϕ
None	0.001	0.001	0.001
Mn(II)	0.036 (36)	0.039 (39)	0.032 (32)
Fe(II)	0.082(82)	0.091 (91)	0.093 (93)
Co(II)	0.085 (85)	0.101 (101)	0.097 (97)
Ni(II)	0.037 (37)	0.044 (44)	0.062 (62)
Cu(II)	0.162 (162)	0.153 (153)	0.225 (225)
Zn(II)	0.201 (201)	0.217 (217)	0.251 (251)
Cd(II)	0.071 (71)	0.075 (75)	0.077 (077)
Ag(I)	0.146 (146)	0.126 (126)	0.118 (118)
Hg(II)	0.231 (231)	0.378 (378)	0.503 (503)
Pb(II)	0.106 (106)	0.102 (102)	0.108 (108)
H^+	0.136 (136)	0.287 (287)	0.467 (467)

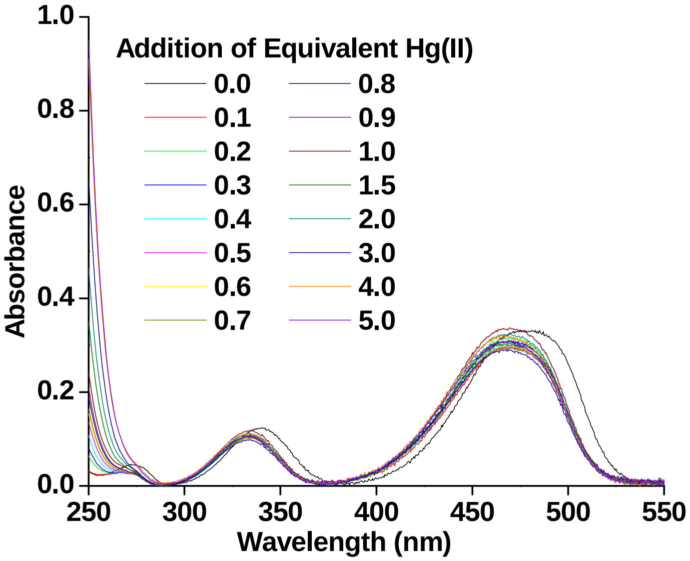

Fig. S16: Absorption spectra of $\mathbf{L_1}$ in presence of increasing concentration of Hg(II) ionic inputs in MeCN.

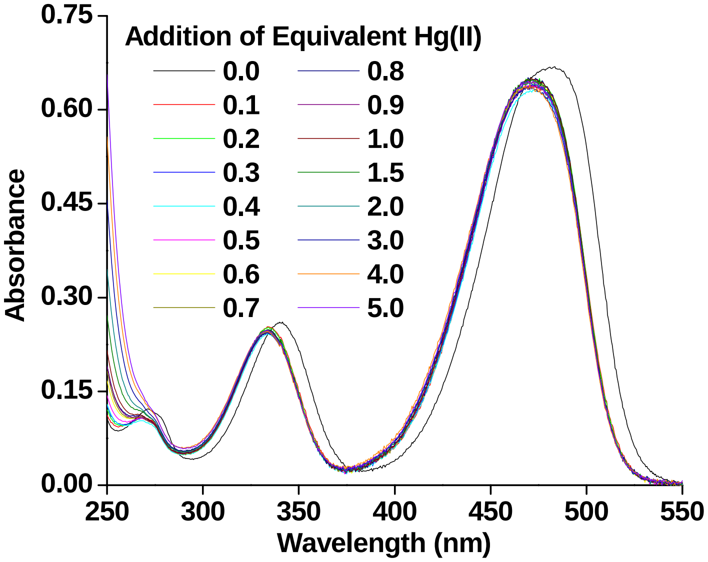

Fig. S17: Absorption spectra of $\mathbf{L_2}$ in presence of increasing concentration of Hg(II) ionic inputs in MeCN.

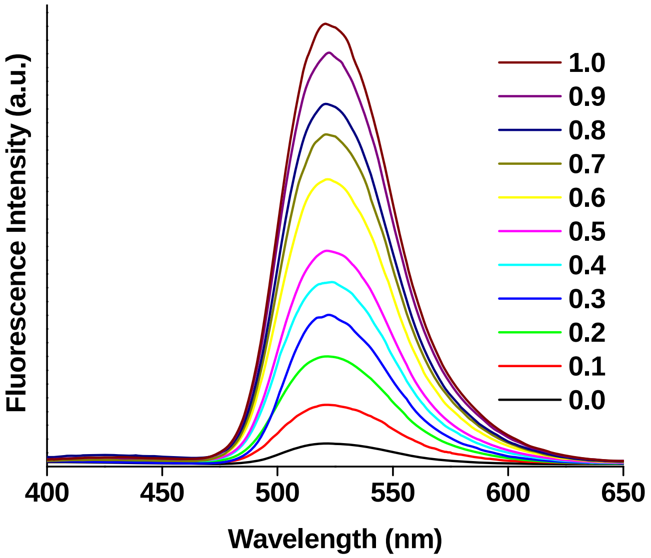

Fig. S18: Absorption spectra of $\mathbf{L_2}$ in presence of increasing concentration of Hg(II) ionic inputs in MeCN.

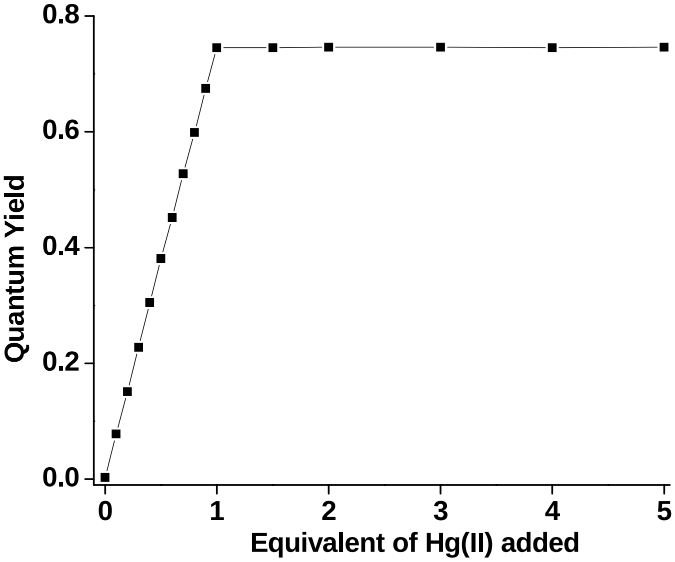

Fig. S19: Plots of fluorescence quantum yield of $\mathbf{L_2}$ as a function of concentration of Hg(II) added in MeCN.

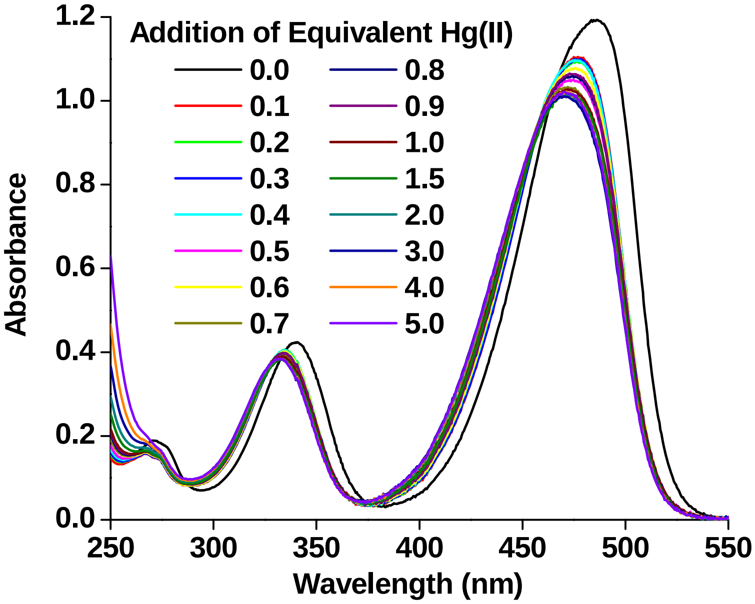

Fig. S20: Absorption spectra of $\mathbf{L_3}$ in presence of increasing concentration of Hg(II) ionic inputs in MeCN.

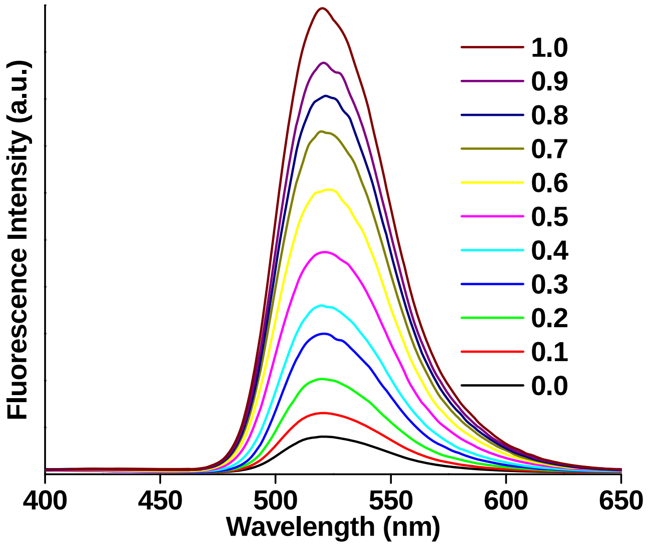

Fig. S21: Absorption spectra of $\mathbf{L_3}$ in presence of increasing concentration of Hg(II) ionic inputs in MeCN.

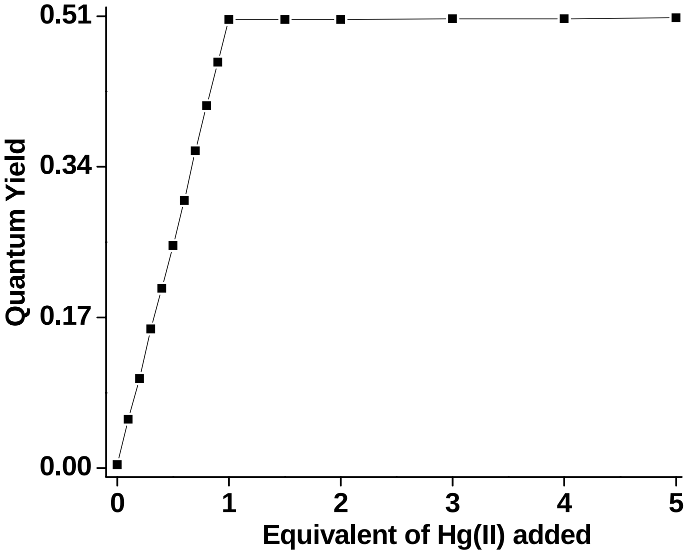

Fig. S22: Plots of fluorescence quantum yield of $\mathbf{L}_3$ as a function of concentration of Hg(II) added in MeCN.

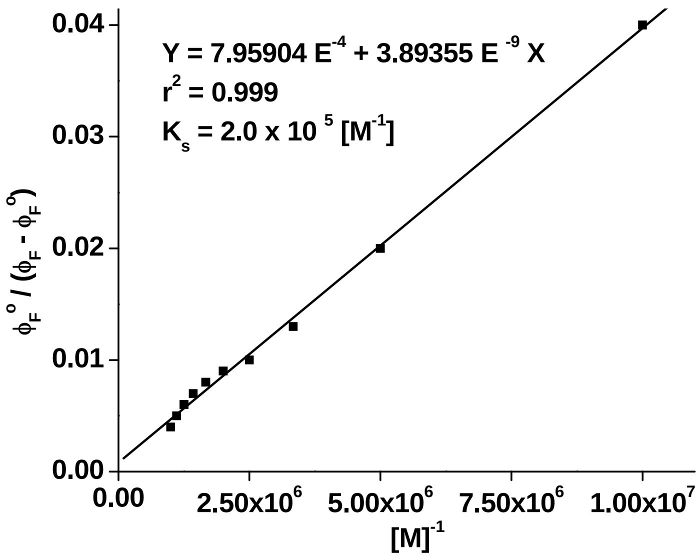

Fig. S23: Linear regression plots for complex stability constant determination of $\mathbf{L}_2$ in presence of Hg(II) as ionic input in MeCN.

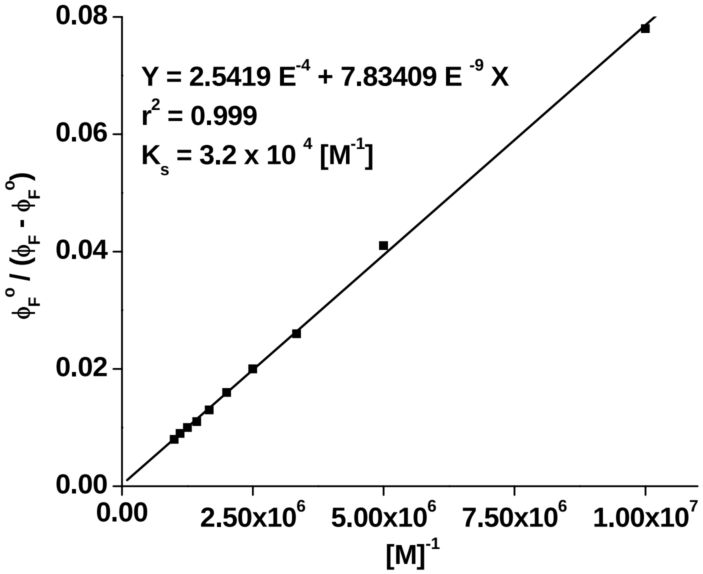

Fig. S24: Linear regression plots for complex stability constant determination of $\mathbf{L_3}$ in presence of Hg(II) as ionic input in MeCN.

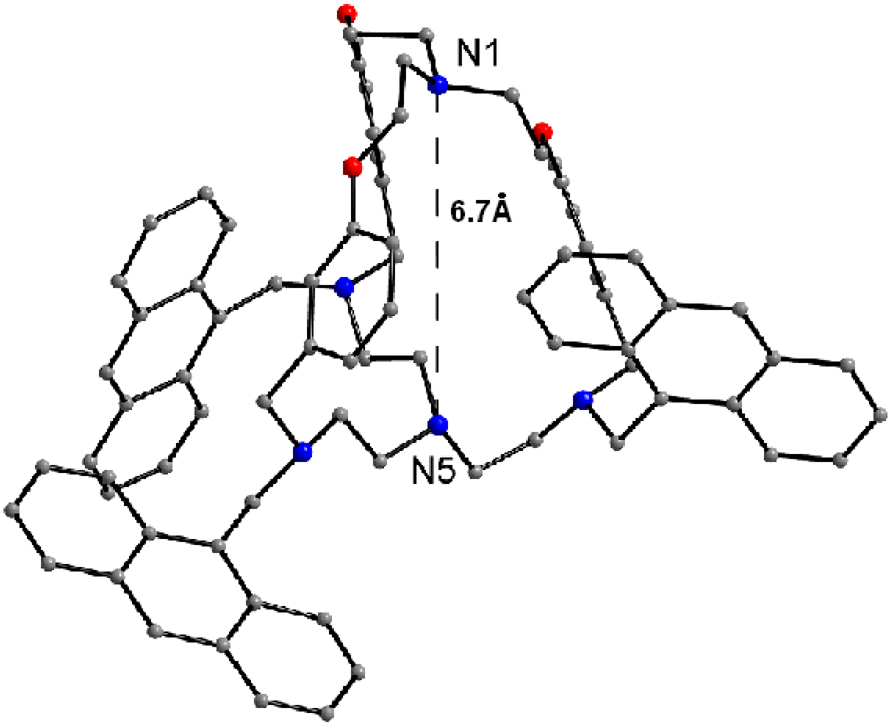

FigS25: Crystal Structure of $\mathbf{L_{12}}$

Table ST8. Crystal data and structure refinement for $\mathbf{L_{12}}$

Empirical formula	C78 H75 N5 O3, 2(C H2 Cl2)
Formula weight	1300.28
Crystal system	Triclinic
Space group	P-1
a, Å	11.970(5)
b, Å	13.569(5)
c, Å	21.610(5)
α(°)	74.456(5)
β(°)	87.681(5)
γ(°)	84.415(5)
V, Å^3	3365(2)
Z	2
ρ_{calc} Mg/m^3	1.283
μ, mm^{-1}	0.230
F(000)	1372
Independent refl.	12899
Refl. used (I>2σ(I))	9016
R_{int} value	0.0353
GOF	0.849
Final R indices [I>2σ(I)]	0.0735
R indices (all data)	0.1004